Performance Analysis of Correlated Massive MIMO Systems with Spatially Distributed Users

Performance Analysis of Correlated Massive MIMO Systems With Spatially Distributed Users

Sudip Biswas, *Student Member, IEEE*, Jiang Xue, *Member, IEEE*, Faheem A. Khan, *Member, IEEE*, and Tharmalingam Ratnarajah, *Senior Member, IEEE*

***Abstract*—In this paper, we analyze the performance of an uplink large-scale multiple-input-multiple-output system with a single base station (BS) serving spatially distributed multiantenna user devices (UDs) within a fixed coverage area. Stochastic geometry is used to characterize the spatially distributed users while large dimensional random matrix theory is used to achieve deterministic approximations of the sum rate of the system. In particular, the users in the vicinity of the BS are considered to follow a Poisson point process within the fixed coverage area. The sum rate of this system is analyzed with respect to different number of antennas at the BS as well as the intensity of the users within the coverage area of the cell. Closed-form approximations for the deterministic rate at low and high signal-to-noise ratio regimes are derived that have very low computational complexity. The deterministic rate for a general *k*th ordered user is also derived. It is shown that the deterministic approximations offer a reliable estimate of the ergodic sum rate obtained by Monte Carlo simulations. We also briefly touch on the growing issue of power consumption in wireless systems by analyzing the energy efficiency of the system using a power consumption model, taking into consideration the circuit power consumption, which is a function of the number of antennas of the BS and UDs.**

***Index Terms*—Energy efficiency, massive multiple-input multiple-output (MIMO), multiuser MIMO, Poisson point process.**

I. Introduction

IN RECENT years, the explosive growth of mobile data traffic has led to an ever-growing demand for much higher capacity, lower latency, and energy efficiency (EE) in wireless networks. It has culminated in the development of the fifth generation (5G) wireless communication systems, expected to be deployed by the year 2020, with key goals of data rates in the range of Gbps, billions of connected devices, lower latency, improved coverage and reliability, and low-cost, energy efficient, and environment-friendly operation.

Massive multiple-input multiple-output (MIMO) is a promising technology for 5G wireless networks that has recently received significant attention to potentially provide a considerable improvement in spectrum and EE [1]–[6]. In this approach, a base station (BS) with very large antenna arrays is used to eliminate intercell interference through highly directional beamforming. Using random matrix theory (RMT), it has been shown that the effects of uncorrelated noise and small-scale fading are eliminated due to very large number of antennas at the BS and the required transmit energy per bit goes to zero as the number of antennas approach to infinity [7]. Moreover, it leads to the use of simpler linear signal processing techniques, such as matched filter precoding/detection to achieve the above advantages. Recently, there has been a flurry of research activities to find out the signal processing and information theoretic limits of massive MIMO systems. In [8] and [9], it is shown that every single-antenna user in a massive MIMO system can scale down its transmit power proportional to the number of antennas at the BS with perfect channel state information (CSI), while the transmit power scales down proportional to the square root of the number of BS antennas with imperfect CSI to get the same performance as a corresponding single-input-single-output (SISO) system. This results in significant improvements in EE for future wireless networks [5], [6]. On the other hand, massive MIMO systems could significantly extend the range of operation compared with a single-antenna system if adequate transmit power is available.

However, the presence of large number of antennas in the system makes it difficult to carry out the exact performance analysis of such a system due to the complexity of the resulting analytical expressions. For this reason, large dimensional RMT [10] has been recently used as a powerful tool to deal with massive MIMO systems. These techniques were first used in [11] and [12] for the analysis of MIMO ergodic capacities. Capacity expressions for infinite antennas with uncorrelated channels were derived for code-division multiple-access codes in [13], and for multiple-antenna systems in [14]. While the reliability of large-scale MIMO systems was studied in [15], an infinite antenna number capacity was calculated with spatially uncorrelated channels and uncorrelated interferers in [16]. In [17], a method was developed to analytically calculate the capacity of spatially correlated channels for large but finite antenna numbers. Furthermore, a deterministic equivalent of ergodic sum rate and an algorithm for evaluating the capacity-achieving input covariance matrices for the uplink large-scale MIMO antenna channels were proposed in [18] and [19].

A stochastic geometry approach has recently gained significant attention to develop tractable models to analyze the performance of wireless networks [20]. In this approach, the wireless network is abstracted to a convenient point process that is used to capture the wireless network properties. A Poisson point process (PPP) is the most popular and tractable point process to model the locations of users and BSs in wireless networks. Inspired by

Manuscript received January 08, 2016; revised April 11, 2016 and July 15, 2016; accepted July 19, 2016. This work was supported by the 7th Framework Programme for Research of the European Commission under Grant HARP-318489 and ADEL-619647. The work of T. Ratnarajah was supported by the U.K. Engineering and Physical Sciences Research Council (EPSRC) under Grant EP/L025299/1. *(Corresponding author: Jiang Xue.)*

The authors are with the Institute for Digital Communications, University of Edinburgh, Edinburgh EH9 3JL U.K. (e-mail: sudip.biswas@ed.ac.uk; j.xue@ed.ac.uk; faheem.khan@ed.ac.uk; T.Ratnarajah@ed.ac.uk).

Digital Object Identifier 10.1109/JSYST.2016.2594155

the stochastic geometry approach to analyze the performance of large-scale MIMO systems, we consider the uplink of such a system with a single BS serving spatially distributed multiple-antenna users within a fixed coverage area of a densely built up urban environment. In such an environment, it is quite hard to find dominant propagation of the signals along the line of sight (LOS). Hence, it is quite reasonable in such a scenario to consider a Rayleigh faded channel with no LOS. We consider the stochastic geometry approach to characterize the spatially distributed users while large dimensional RMT is used to achieve deterministic approximations of sum rate of the system. It is assumed that the users in the cell follow a PPP. We then analyze the sum rate of this system with respect to varying number of antennas at the BS as well as the intensity of the users within the coverage area of the cell. Closed-form expressions for the low signal-to-noise ratio (SNR) and high SNR regimes are also provided. At this point, we would like to note that our results complement the contribution of [19]. However, we consider the more general and realistic case in which the stochastic nature of the users and their individual path losses are considered.

Furthermore, we briefly analyze the EE of such systems, which is currently one of the primary design goals of any wireless communication system. EE of a communication link is usually defined as the total energy required for transmission in order to achieve a specific spectral efficiency [8], [21]. The significance of the total power consumption in MIMO systems has been emphasised in [22]. MIMO systems have been stated to offer improved EE on account of array gains and diversity effects [2]. Hence, the definition of EE can be quite delusive at times especially when a massive MIMO scenario is considered with the number of antennas increasing asymptotically leading toward unbounded EE, which is quite improbable for practical systems. In [23], the effect of the number of BS antennas on EE has been discussed, while [24] discusses about designing optimal EE for massive MIMO systems. In our analysis, we take into consideration, the circuit power consumption of both the BS and the user equipments (UEs) accordingly form an EE expression that varies with the number of BS antennas and the users.

The main contributions of this paper can be summarized as in the following points.

1) We have presented approximations of the sum rate of a single-cell multiuser MIMO system with large number of antennas at BS and multiple antennas at UEs. This is adhering to the consideration that the users follow a PPP within the cell.
2) We have considered correlated Rayleigh fading and uniformly distributed UEs within the cell and power-law path loss. The path loss exponent determines the large-scale fading of the users.
3) We have provided high and low SNR approximations of the sum rate of the system that can be considered as good low complexity approximations of the analytical capacity.
4) We have also provided the approximate sum rate for the kth ordered user.
5) We also touch on the analysis of the EE of the whole system considering a realistic power consumption model that includes the circuit power consumption of the system.

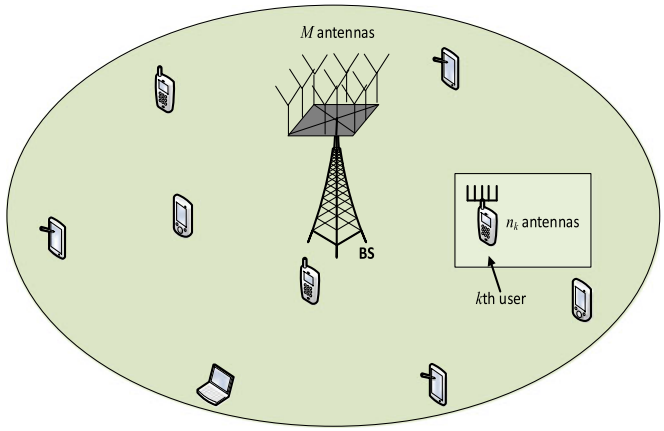

Fig. 1. Illustration of a multiuser MIMO setup with multiple antennas both at the BS and users. The users are uniformly distributed within the cell.

Notations: We use upper and lower case boldface to denote matrices and vectors, respectively. $\mathbb{R}$ denotes the real plane, while $\mathbb{C}$ the complex plane. The expectation operator is denoted by $\mathbb{E}\{\cdot\}$ and the probability by $\mathbb{P}[\cdot]$. $(\cdot)^*$ and $(\cdot)^H$ denote the transpose and Hermitian transpose of vectors/matrices, respectively, while $\mathrm{tr}(\cdot)$ and $|\cdot|$ denote the trace and determinant of a matrix, respectively. A complex normal variable with mean μ and variance σ^2 is given as $\mathcal{CN}(\mu, \sigma^2)$. Last $\langle \mathbf{A} \rangle$ returns the submatrix of $\mathbf{A}$ obtained by extracting the elements of the rows and columns with indices from $\sum_{i=1}^{k-1} n_i + 1$ to $\sum_{i=1}^{k} n_i$, and $\mathrm{eig}(\mathbf{A})$ returns the eigenvalues of the matrix $\mathbf{A}$. All other symbols will be explicitly mentioned wherever used.

The rest of the paper is organized as follows. Section II describes the system model. The mathematical preliminaries used in determining the closed-form approximations are presented in Section III. Section IV provides the sum-rate analysis. In Section V, low and high SNR approximations of sum rate are derived. The capacity of the kth ordered user is found in Section VI, while Section VII presents an analysis on EE of the system. In Section VIII, we provide the numerical analysis followed by the conclusion of the paper in Section IX.

II. System Model

We consider the uplink of a single-cell multiuser MIMO Multiple Access Channel (MAC) system consisting of a BS with M antennas, receiving signals from K users, each equipped with $n_1, \ldots, n_K$ antennas, respectively. A schematic illustration[1] of the system under consideration is given in Fig. 1. Considering a separable correlation model for analytical tractability, we model the $M \times n_k$ channel, $\mathbf{W}_k$ between the BS and the kth user as

$$\mathbf{W}_k = \mathbf{H}_k ||\mathbf{x}_k||^{-\frac{\alpha}{2}}, \tag{1}$$

with

$$\mathbf{H}_k = \mathbf{R}_k^{\frac{1}{2}} \mathbf{G}_k \mathbf{T}_k^{\frac{1}{2}}, \tag{2}$$

[1]We consider a circular cell of radius r in $\mathbb{R}^2$ with an area of πr^2. A hexagonal cell in $\mathbb{R}^2$ can also be considered. The radius of the cell, r can then be considered from the center to the vertex and the area (considering a regular hexagon with side b) is given as $3b\sqrt{r - \frac{b^2}{4}}$.

where $\mathbf{R}_k^{\frac{1}{2}}$ and $\mathbf{T}_k^{\frac{1}{2}}$ are $M \times M$ and $n_k \times n_k$ deterministic receive and transmit correlation matrices, respectively. Here, $\mathbf{G}_k \in \mathbb{C}^{M \times n_k}$ consists of complex random identically independently distributed (i.i.d) variables with zero mean and unit variance that models independent fast fading. We assume that the users do not have any LOS with the BS and hence, $\mathbf{G}_k$ is Rayleigh-faded. The separable model allows us to keep the correlation between any two transmitting antennas to be fixed irrespective of the receiving antenna and vice versa. Moreover, $\mathbf{x}_k \in \mathbb{R}^2$ denotes the physical location (distance between the UE and the centre of the cell) of the kth user in meters and it is computed with respect to the BS. The large-scale fading at a specific user location is described by the function $\mathcal{F}(\cdot) : \mathbb{R}^2 \rightarrow \mathbb{R}$. Thus, the average channel attenuation due to path loss and shadowing[2] at user location $\mathbf{x}_k$ can be represented by $\mathcal{F}(\mathbf{x}_k)$. The large-scale fading is assumed to be independent over M and also constant over many coherence time intervals. This assumption is quite reasonable due to the fact that the distances between the users and the BS are much larger than the distance between the antennas at the BS. Also, α in (1) denotes the path loss exponent varying from 2 to 4, with 2 denoting a free space propagation and 4 a relatively lossy environment.

Let r denote the radius of the circular cell and $x = ||\mathbf{x}||$. The user locations can be described by the probability density function as

$$f(\mathbf{x}) = \begin{cases} \frac{2x}{r^2}, & 0 \leq x \leq r \\ 0, & \text{otherwise.} \end{cases} \tag{3}$$

Furthermore, we model the large-scale fading as

$$\mathcal{F}(\mathbf{x}) = x^{-\frac{\alpha}{2}}, \quad \text{for} \;\; x > 0, \tag{4}$$

which is then put together with the fast fading as shown in (1).

In this paper, considering a typical BS at the origin of the cell, we use a homogeneous PPP, $\mathbf{\Phi}(\mathbf{x}) \subset \mathbb{R}^{\mathbf{2}}$ with intensity κ to model the locations of the users on the plane. The number of users, K is a function of κ. $\mathcal{F}(\mathbf{x}_k)$ is a key requisite in all our subsequent discussions throughout the paper. Assuming the average transmitted power of each user to be equal, the $M \times 1$ received vector at the BS can now be expressed as

$$\mathbf{y} = \sqrt{p} \sum_{k \in \mathbf{\Phi}(\mathbf{x})} \mathbf{W}_k \mathbf{u}_k + \mathbf{z}, \tag{5}$$

where $\sqrt{p}\mathbf{u}_k$ is the $n_k \times 1$ vector of symbols transmitted by the kth user, with $p = \frac{P}{K}$ denoting the average transmitted power of each user and $\mathbf{z}$ a vector of additive white Gaussian noise[3] with zero mean and covariance $\sigma^2 \mathbf{I}_M$. P is the total transmitted power of all the users and is considered to be fixed.

[2]The results in this paper can also be extended for more complicated fading models while incorporating shadowing effects. For example, adding log-normal shadowing to the corresponding results is straightforward and can be done by modifying (1) as $\mathbf{W}_k = \mathbf{H}_k \beta_k / \|\mathbf{x}_k\|^{\frac{\alpha}{2}}$, where β_k is a log-normal random variable with standard deviation σ_{shadow}.

[3]We would like to note that in this work interference from adjacent cells are not considered.

III. Assumptions and Preliminaries

In this section, we state the necessary assumptions that will be used throughout the paper.

1) Perfect Channel State Information: Throughout the paper, we assume that the channel matrices $\{\mathbf{W}_k\}_{\forall k}$ are perfectly known at the BS.
2) SNR: We assume for each transmission link $G_{k_{ji}}$ that $\mathbb{E}\{|G_{k_{ji}}|^2\} = 1$. When only transmit antenna i is active, the instantaneous received SNR at the receiving antenna j is $\frac{p|G_{k_{ji}}|^2}{\sigma^2}$. Thus, the effective transmit SNR for the communication link can be given as $\rho = \frac{p}{\sigma^2}$. For analytical convenience, we set the same noise level (σ^2) at all the antennas, though this is not mandatory. The performance analyzes performed in the following sections will mostly be as a function of ρ.
3) $\mathbf{R}_k$ and $\mathbf{T}_k$ are deterministic and nonnegative definite and are normalized as
$$\begin{aligned} \text{tr}(\mathbf{R}_k) &= M \\ \text{tr}(\mathbf{T}_k) &= n_k. \end{aligned} \tag{6}$$
4) Empirical and limiting spectral distribution: Let $\mathbf{A}_M \triangleq \sum_{k \in \mathbf{\Phi}(\mathbf{x})} \mathbf{W}_k \mathbf{W}_k^H$. Without loss of generality, the mutual information of a MIMO channel can be associated with the eigenvalues of the matrix $\mathbf{A}_M$ [25]. According to RMT, the empirical spectral distribution of the eigenvalues, λ of $\mathbf{A}_M$ can be given as
$$\mu_{\mathbf{A}_M}(\lambda) = \frac{1}{M}[\text{number of eigenvalues of } \mathbf{A}_M \leq \lambda]. \tag{7}$$
Before we proceed any further, it is worth mentioning the contribution of [18] and [19]. A deterministic equivalent of the ergodic mutual information for Rician faded Kronecker MIMO channel was found by Zhang *et al.* using the Shanon transform. This is better elucidated as Lemma 2 in Appendix A. While it has been a constant endeavor of researchers to study the limit of the empirical distribution, also known as limiting spectral density (LSD), μ_M of $\mathbf{A}_M$, [18] and [19] do that with the help of Stieltjes transform of $\mu_{\mathbf{A}_M}$ defined as
$$\begin{aligned} S_{\mathbf{A}_M}(z) &\triangleq \left[\int_{\mathbb{R}^+} \frac{1}{\lambda - z} \mathrm{d}\mu_{\mathbf{A}_M}(\lambda)\right]_{\forall z \in \mathbb{R}^+} \\ &= \frac{1}{M} \text{tr}(\mathbf{A}_M - z\mathbf{I}_M)^{-1}. \end{aligned} \tag{8}$$
Furthermore, with the help of Stieltjes transform it was shown that
$$\mu_{\mathbf{A}_M}(\lambda) - \mu_M(\lambda) \xrightarrow{a.s.} 0, \tag{9}$$
which was accordingly used to find a deterministic equivalent of the ergodic mutual information. Let $\mathcal{R}_{\mathbf{A}_M}$ represent the ergodic sum rate of a MIMO MAC and $\mathcal{R}_M$ its deterministic equivalent. It was then shown that $\mathcal{R}_{\mathbf{A}_M} - \mathcal{R}_M \xrightarrow{a.s.} 0$.

More detailed explanation about the relation between Stieltjes and Shanon transforms can be found in [10]. However, the analysis based on Stieltjes and Shanon transforms is not

straightforward and can be quite complex. Hence, we find the approximation of the ergodic sum rate for the case of correlated Rayleigh faded channels, where we use stochastic geometry to characterize the distribution of the users within the cell. We will show that this approximation is indeed tight. As mentioned previously, the users follow a PPP, $\mathbf{\Phi}(\mathbf{x})$ with intensity κ. Furthermore, we also provide two low complexity approximations based on high and low SNRs.

IV. Sum-Rate Analysis

For very large MIMO systems, when both $M, K \to \infty$, it becomes increasingly difficult to analyze the performance of the system based on exact analytical expressions, as they are often too complicated to evaluate. Even computer simulations can be quite demanding for systems with such large dimensions. In such cases, large RMT can help to develop approximate analytical expressions, which substantially reduce the computational complexity. Accordingly, in this section, we formulate the approximate ergodic sum rate of the system under consideration.

A. Deterministic Sum Rate

Let $\mathbf{\Xi_k}$ be the covariance matrix of the transmitted vectors, $\mathbf{u}_k$ of the kth user such that

$$\mathbb{E}\{\mathbf{u}_k \mathbf{u}_l^*\} = \begin{cases} \mathbf{\Xi_k}, & \text{if } \mathbf{l} = \mathbf{k} \\ 0, & \text{otherwise} \end{cases} \tag{10}$$

and

$$\mathbf{T}_k = \mathbf{T}_k^{\frac{1}{2}} \mathbf{\Xi_k} \mathbf{T}_\mathbf{k}^{\frac{1}{2}}. \tag{11}$$

$\mathbf{\Xi_k}$ can be easily optimized for the case of Rayleigh i.i.d channel as $\mathbf{I}_{n_k}$. This is due to the consideration that $\mathbf{u}_k$ are independent and have the same transmit power. The ergodic sum rate of such a MIMO MAC can be given as[4] [26], [27]

$$\mathcal{R}_{\mathbf{A}_M}(\rho) \equiv \frac{1}{M} \mathbb{E}_{\mathbf{H}} \left\{ \log\det\left(\mathbf{I}_M + \rho \mathbf{A}_M\right) \right\}, \tag{12}$$

where $\rho = \frac{p}{\sigma^2}$ is the transmit SNR of the system as described earlier and $\mathbf{A}_M$ is as discussed in the previous section. Considering the properties of a PPP, $\sum_{k \in \mathbf{\Phi}(\mathbf{x})} n_k \to \infty$ for some specific probability. Furthermore, we focus on a single BS receiver with multiple antennas such that $M \to \infty$, which receives signals from multiple users. At this point, we stress that while the original massive MIMO definition in [7] assumed that $\frac{M}{K} \gg 1$, we consider the more general definition from [3], where $\frac{M}{K}$ can also be a small constant. Henceforth, we aim to show that $\mathcal{R}_{\mathbf{A}_M} - \mathcal{R}_M \xrightarrow{a.s.} 0$, where $\mathcal{R}_{\mathbf{A}_M}$ is computed through simulations and $\mathcal{R}_M$ through analytical approximations, which is validated in Section VIII of numerical results.

Lemma 1: For a single-cell massive MIMO system following a PPP in $\mathbb{R}^2$, the general probability of finding K users within the coverage area of the cell can be given as [28]

$$\mathbb{P}[K \text{users in the cell}] = \exp\{-\kappa\mu(A)\} \frac{(\kappa\mu(A))^K}{K!}, \tag{13}$$

where κ is the intensity and $\mu(A)$ is the standard Lebesgue measure of a bounded Borel $A \subset \mathbb{R}^2$, which is formed by the topological space of the cell.

Now, leveraging the results of [19, sec. III.A], for the system model in consideration, the capacity of the system can be approximated as the following proposition.

Proposition 1: The ergodic sum rate of a massive MIMO system based on LSD of $\mathbf{A}_M$ can be approximated as

$$\begin{aligned} \mathcal{R}_M(\rho) = & \frac{1}{M} \log\det\left(\mathbf{I}_M + \sum_{k=0}^{\infty} \tilde{\epsilon}_k(\rho) \mathbf{R}_k \ \mathbb{P}(k)\right) \\ & + \frac{2}{\alpha M \ln 10} \sum_{k=0}^{\infty} \sum_{i=1}^{n_k} G_{3,3}^{2,2}\left(\frac{r^\alpha}{\psi_k \lambda_{ki}} \middle| \begin{matrix} 1-\frac{2}{\alpha}, 0, \ 1 \\ 0, \quad 0, -\frac{2}{\alpha} \end{matrix} \right) \\ & \times \mathbb{P}(k) - \sum_{k=0}^{\infty} \epsilon_k(\rho) \tilde{\epsilon}_k(\rho) \ \mathbb{P}(k) \end{aligned} \tag{14}$$

Here,

$$\epsilon_k(\rho) = \frac{1}{M} \mathrm{tr}\left(\rho \mathbf{R}_k \left[\mathbf{I}_M + \sum_{k=0}^{\infty} \tilde{\epsilon}_k(\rho) \mathbf{R}_k \ \mathbb{P}(k) \right]^{-1} \right), \tag{15}$$

$$\tilde{\epsilon}_k(\rho) = \frac{1}{n_k} \mathrm{tr}\left(\rho \mathbf{T}_k \left\langle \mathrm{diag}\left[\mathbf{I}_{n_k} + \frac{M \epsilon_k(\rho) \mathbf{T}_k}{n_k} \right]^{-1}_{\forall k \in \mathbf{\Phi}(\mathbf{x})} \right\rangle \right), \tag{16}$$

$G_{p,q}^{m,n}\{\cdot\}$ is the hyper-geometric function also known as Meijer G-function [29, eq. (9.301)] and $\lambda_{ki} = \mathrm{eig}(\mathbf{T}_k)$. There is a unique solution to (15) and (16) for $\rho \in \mathbb{R}^+$, where $\epsilon_k(\rho) \in \mathbb{S}(\mathbb{R}^+)$ and $\tilde{\epsilon_k}(\rho) \in \mathbb{S}(\mathbb{R}^+)$ for $k \in \mathbf{\Phi}(\mathbf{x})$. Furthermore, $\mathbb{S}(\mathbb{R}^+)$ can be interpreted as the class of all Stieltjes transforms of finite positive measures carried over $\mathbb{R}^+$ and $\mathbb{P}(k)$ is obtained from Lemma 1.

Proof: It is to be noted that, the number of users as mentioned before is decided based on a PPP and calculated with respect to the probability given by Lemma 1 and the intensity of the users, κ. Our aim now is to derive the closed form expression of the deterministic ergodic sum rate as given in (14) and also to show that there is a unique solution to (15) and (16). For better understanding, we divide the proofs into two parts. The detailed derivation of (14) is given in Appendix B, while the proof of uniqueness of (15) and (16) is given in Appendix C. ■

V. High and Low SNR Sum-Rate Approximations

A. High SNR Regime

Fast fading channels have the same properties at high SNR as time-invariant channels, irrespective of the knowledge of channel state information at transmitter. In this section, we analyze the capacity in the high SNR regime, i.e., $\rho \to \infty$.

Corollary 1: Let $\psi_k = \frac{M}{n_k} \epsilon_k(\rho)$. Then at relatively high SNR ($\rho \to \infty$) regime for correlated massive MIMO channels, $\mathcal{R}_\mathcal{M}$

[4] We assume a maximum likelihood sequence estimator at the BS to separate different data streams.

approaches the exact sum rate and can be derived as

$$\begin{aligned}\mathcal{R}_{\mathcal{M}_{\rho\to\infty}}(\rho) = \; & \frac{1}{M}\sum_{k=0}^{\infty}\log(\mathrm{tr}(\tilde{\epsilon}_k(\rho)\mathbf{R}_k))\mathbb{P}(k) \\ & + \frac{1}{2}\sum_{k=0}^{\infty}\sum_{i=1}^{n_k}\left[2\log(\psi_k\lambda_{k\,i}) + \left(2\log(r^{-\alpha})\right.\right. \\ & \qquad \left.\left. + \alpha\right)\right]\mathbb{P}(k) \\ & - \sum_{k=0}^{\infty}\epsilon_k(\rho)\tilde{\epsilon}_k(\rho)\;\mathbb{P}(k). \end{aligned} \tag{17}$$

Proof: Considering ρ to be large, (14) can be approximated as

$$\begin{aligned}\mathcal{R}_{\mathcal{M}_{\rho\to\infty}}(\rho) = \; & \frac{1}{M}\log\det\left(\sum_{k=0}^{\infty}\tilde{\epsilon}_k(\rho)\mathbf{R}_k\right)\mathbb{P}(k) \\ & + \frac{2}{r^2}\sum_{k=0}^{\infty}\left(\sum_{i=1}^{n_k}\int_0^r \log(\psi_k\lambda_{k\,i}x^{-\rho})x\mathrm{d}x\right)\mathbb{P}(k) \\ & - \sum_{k=0}^{\infty}\epsilon_k(\rho)\tilde{\epsilon}_k(\rho)\;\mathbb{P}(k). \end{aligned} \tag{18}$$

Using integration by parts and substituting the limits of the integral, we obtain (17). ■

B. Low SNR Regime

When the SNR of the system is relatively low, the multiplexing gains of the system are lost. In such a scenario when $\rho \to 0$, the sum rate can be approximated by the following corollary.

Corollary 2: At low SNR the sum rate can be approximated as

$$\begin{aligned}\mathcal{R}_{\mathcal{M}_{\rho\to 0}} = \; & \sum_{k=0}^{\infty}\left[\frac{1}{M}\frac{\mathrm{tr}(\tilde{\epsilon}_k(\rho)\mathbf{R}_k)}{\log 10}\right. \\ & \left. + \; \frac{2r^{1-\alpha}\mathrm{tr}(\psi_k\mathbf{T}_k)}{(2-\alpha)M\log 10}\right]\mathbb{P}(k). \end{aligned} \tag{19}$$

Proof: This can be easily proved by using the approximation $\log_2(1+x) \approx x/\log 2$ for small x in (14). ■

C. Complexity Analysis

In this section, we analyze the complexity of both the high and low SNR approximations with respect to (14). We focus on the complexity of calculation and running time for common mathematical operations that are used in our algorithms. Complexity, in this analysis refers to the time complexity of performing computations with respect to a reference Turing machine [30].

We consider the upper bound of the operation time such that for a sufficiently large number n, the limiting behavior of a function $f(n)$ is denoted by $O\left(g(n)\right)$, where the function f is bounded above by the function g. Let the complexity of ϵ_k and $\tilde{\epsilon}_k$ be denoted by $O(\phi_1)$ and $O(\phi_2)$. Then, following the complexity of some basic mathematical calculations as given in [31], for a single iteration under $\mathbf{\Phi}(\mathbf{x})$, the complexity of the approximation in Proposition 1, Corollary 1 and Corollary 2 can be approximated as $O(n^3\log n + n^2(\log n)^2 + \phi_1\phi_2)$, $O(n^2\log n + \log n + \phi_1\phi_2)$, and $O(n^2)$, respectively. Hence, it can be stated that the high and low SNR approximations have low computational complexities when compared to the sum-rate approximation given in Proposition 1. Later, in the numerical section of the paper, we show that these two approximations are quite tight and can be used appropriately in the respective regimes.

VI. General User Capacity

We have so far focused our discussion based on the total number of users, K, within the coverage area of the BS. We now order the users based on their distances from the BS as $||\mathbf{x}_1|| < ||\mathbf{x}_2|| < ||\mathbf{x}_3|| < \ldots < ||\mathbf{x}_{k\in\mathbf{\Phi}(\mathbf{x})}|| < \cdots$. In this section, we discuss the capacity of the kth order user selected from the PPP based on the probability, $\mathbb{P}$ and intensity, κ.

Proposition 2: Considering the order of the users as described, the distribution of the location of the kth ordered user with respect to the BS can be given as

$$f(||\mathbf{x}_k||) = \exp(-\kappa\pi r^2)\frac{2(\kappa\pi r^2)^k}{r\Gamma(k)}. \tag{20}$$

The ergodic rate for this user can now be approximated as

$$\begin{aligned}\mathcal{R}_M^k(\rho) = \; & \frac{1}{M}\log\det\left(\mathbf{I}_M + \tilde{\epsilon}_k(\rho)\mathbf{R}_k\right) \\ & + \sum_{n=0}^{\infty}\frac{2(-1)^n(\sqrt{\kappa\pi})^{(2n+k)}r^{(2(n+k)+1)}}{\alpha n!\Gamma(k)} \\ & \times\sum_{i=1}^{n_k}G_{3,3}^{2,2}\left(\frac{r^\alpha}{\psi_k\lambda_{k\,i}}\middle|\begin{matrix}1-\frac{2(n+k)+1}{\alpha}, 0, & 1\\ 0, & 0, -\frac{2(n+k)+1}{\alpha}\end{matrix}\right) \\ & -\epsilon_k(\rho)\tilde{\epsilon}_k(\rho), \end{aligned} \tag{21}$$

where $n \in \mathbb{R}$ and $0 \le n \le \infty$.

Proof: To prove this, we build on our previous proof of (14) and consider any one particular user. The detailed derivation is given in Appendix D.

Corollary 3: Considering the order of the users as described, the distribution of the first user in the order can be given as

$$f(||\mathbf{x}_1||) = 2\exp(-\kappa\pi r^2)\kappa\pi r, \tag{22}$$

Accordingly, the rate for this user can be approximated as

$$\begin{aligned}\mathcal{R}_M^1(\rho) = \; & \frac{1}{M}\log\det\left(\mathbf{I}_{\mathrm{M}} + \tilde{\epsilon}_1(\rho)\mathbf{R}_1\right) \\ & + \sum_{n=0}^{\infty}\frac{2(-1)^n(\sqrt{\kappa\pi})^{(2n+1)}r^{(2(n+1))}}{\alpha n!} \\ & \times\sum_{i=1}^{n_k}G_{3,3}^{2,2}\left(\frac{r^\alpha}{\psi_1\lambda_{1\,i}}\middle|\begin{matrix}1-\frac{2(n+1)}{\alpha}, 0, & 1\\ 0, & 0, -\frac{2(n+2)}{\alpha}\end{matrix}\right) \\ & -\epsilon_1(\rho)\tilde{\epsilon}_1(\rho). \end{aligned} \tag{23}$$

VII. Energy Efficiency

The EE of a communication link is the ratio of the achievable sum rate to the total power consumed and is given in bits/joule [8], [21]. The corresponding EE as studied in many existing works is thus given as [8], [24], [32]

$$\xi = \frac{\mathcal{R}_M}{p^{\text{PA}} + p^{\text{RF}}} \tag{24}$$

where p^{PA} is the power consumed by the power amplifiers and p^{RF} is the power consumed by the RF components of both BS and UEs.

A. Power Amplifiers

The average power in watt consumed by the power amplifiers during uplink can be approximated as [24], [26]

$$p^{\text{PA}} = P(\alpha + 1) \tag{25}$$

where $\alpha = \frac{\zeta}{\eta} - 1$ with ζ being the modulation-dependent peak to average power ratios for uplink, while η is the power amplifier efficiency and P is the total transmitted power of all users as described earlier.

B. RF Chains

The average power in watt consumed in the RF chains for a typical MIMO transmitter–receiver set can be given as [21]

$$p^{\text{RF}} = Mp^{\text{BS}} + Kp^{\text{UE}} \tag{26}$$

where p^{BS} is the power required at the BS to run the circuit components and p^{UE} is the power associated with the UEs. They are further defined as follows:

$$p^{\text{BS}} = p^{\text{BS}}_{\text{mix}} + p^{\text{BS}}_{\text{filt}} + p^{\text{BS}}_{\text{ADC}} + p^{\text{BS}}_{\text{DAC}} + p^{\text{BS}}_{\text{OSC}} \tag{27}$$

$$p^{\text{UE}} = p^{\text{UE}}_{\text{mix}} + p^{\text{UE}}_{\text{filt}} + p^{\text{UE}}_{\text{ADC}} + p^{\text{UE}}_{\text{DAC}} + p^{\text{UE}}_{\text{OSC}} \tag{28}$$

where p_{mix}, p_{filt}, p_{ADC}, p_{DAC}, and p_{OSC} denote the power consumed by the mixers, filters, analog-to-digital converters, digital-to-analog converters, and local oscillator, respectively.[5] Most existing works consider the total power consumed in the RF cicuits of the system to be fixed. This consideration can be very detrimental in the analysis of a large-scale MIMO system, like ours, where both $M,\ K \to \infty$, which eventually leads to unbounded EE. This outcome is the consequence of disregarding the fact that dedicated circuit components with nonzero power consumption are required for each antenna at the BS. As a matter of fact, EE does not always increase with M or K. The simulation results in Section VIII validate this theory and provide further valuable insights into this. In this regard, it is worth mentioning that for our case, we have considered the transmission to be i.i.d, which reduces the requirement of high-complexity optimization of the transmitted power. Furthermore, we have previously assumed that the average power transmitted by all the users is equal. Nevertheless the optimization of power to attain better EE is of paramount importance. While in this paper we have tried to give an appropriate model for p^{RF} and validate our assumptions with simulations, the optimization of the power and other parameters such as M and K to attain a energy efficient system are left for future work.

[5]The components considered in this paper may vary from setups used in practical scenarios. Any other components used can easily be included in the expressions of p^{BS} and p^{UE} while the ones that are not used may be removed.

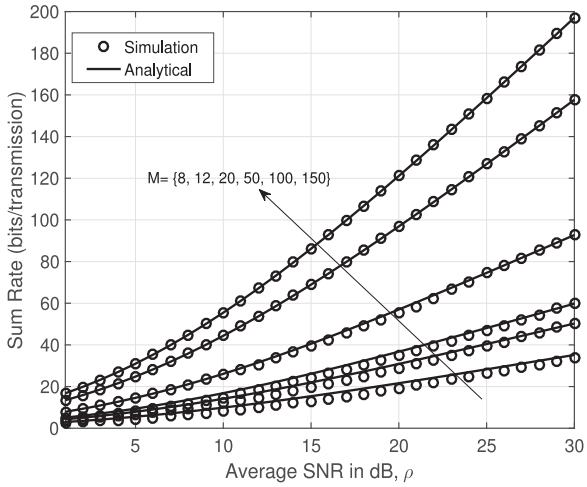

Fig. 2. Simulation and analytical sum rate versus SNR for different number of antennas, M at the BS. $\kappa = 0.01$, $\alpha = 2.2$.

VIII. Numerical Results

This section validates the system model and also verifies our result in Proposition 1 and the resulting corollaries by making comparisons between the ergodic sum rate and the approximate sum rate. We analyze the behavior of the system model under consideration with respect to increasing SNR while varying other significant system parameters. In general, the computation of the ergodic sum rate is done through Monte Carlo simulations, which is then used to validate the simulation of the analytical results. Unless stated otherwise, most of the values of the parameters used are inspired from the literature mentioned in the references. For the system guidelines, we consider a circular cell as stated earlier with a radius of $r = 1000$ m. The users are uniformly distributed within the coverage area of the cell and their numbers are governed by Poisson distribution with intensity κ and probability given by (13) in Lemma 1. Hereinafter, we consider all the users in the system to be equipped with two antennas and examine the validity of our approximations with respect to simulations. While Fig. 2 shows the uplink sum rate versus SNR for various antenna configurations at the BS, Fig. 3 shows the uplink sum rate versus SNR for different user intensities, κ inside the coverage area of the cell. Specifically, these two figures attempt at validating Proposition 1. In other words, we intend to see how well $\mathcal{R}_M(\rho)$ in (14) approximates to $\mathcal{R}_{\mathbf{A}_M(\rho)}$ in (12). Here, we choose the path loss exponent, $\alpha = 2.2$ and the intensity of the users, $\kappa = 0.01$. In Fig. 1, understandably, the sum-rate increases as we increase the average SNR. But what is notable is that, as we increase the number of antennas from 8 to 150, the analytic curve tends to converge tightly toward the simulation. This implies that $\mathcal{R}_M(\rho) - \mathcal{R}_{\mathbf{A}_M(\rho)} \to 0$,

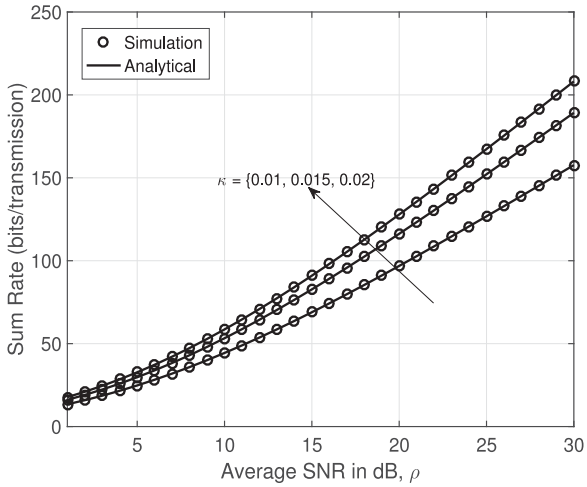

Fig. 3. Simulation and analytical sum rate versus SNR for different intensities, κ of the users within the cell. $M = 100$, $\alpha = 2.2$.

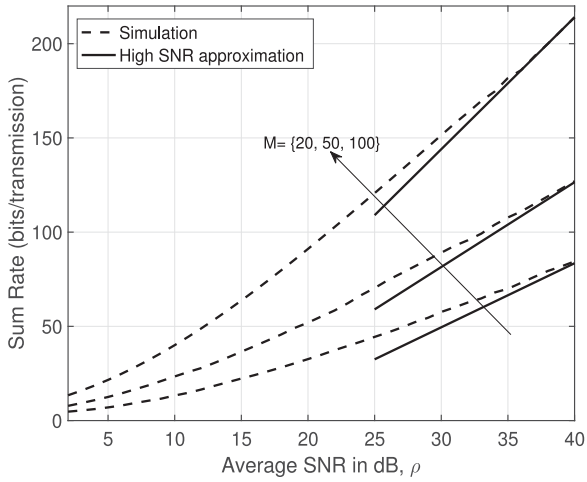

Fig. 4. High SNR approximation of sum rate versus SNR for different number of antennas, M at the BS. $\kappa = 0.01$, $\alpha = 2.2$.

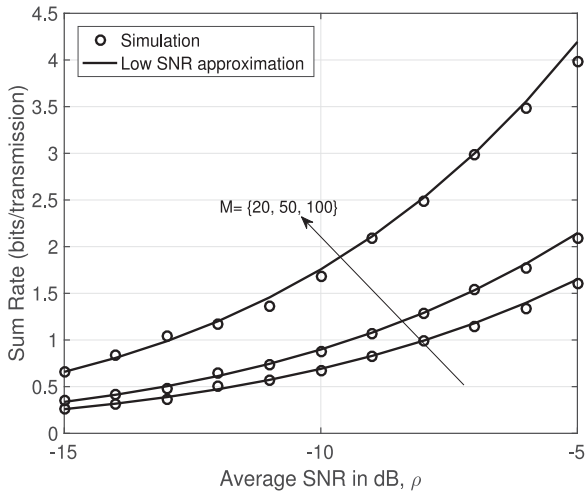

Fig. 5. Low SNR approximation of sum rate versus SNR for different number of antennas, M at the BS. $\kappa = 0.01$, $\alpha = 2.2$.

which proves the validity of our approximation for large MIMO systems. Nevertheless, it is also important to see how the analytical approximation fares when the system dimension is not so large. In this regard, we see that the approximation also holds true for fewer number of antennas as can be seen for the cases of $M = 8, 12, 20, 50$ but with error of a few bits. Hence, it is crucial to investigate the scenarios when the number of antennas is not a very large number, which we concentrate on in our subsequent analyzes. In addition, as we increase M, the ergodic sum rate also increases. For the case of Fig. 3, we choose $M = 100$ and $\alpha = 2.2$. We vary κ from 0.01 to 0.02 in steps of 0.005. Our approximation holds good for all the three cases and hence, we can assert the convergence of our analytic approximation for a massive MIMO scenario. Furthermore, the sum rate of the system increases owing to the increase in κ that in turn increases K, thus increasing the transmit antennas. The increase in sum rate follows a similar pattern as Fig. 2 with the scaling more pronounced when increasing from $\kappa = 0.01$ to 0.015 than 0.015 to 0.02.

Hereinafter, based on the results of Fig. 2, we also focus on the regimes when the system dimension may not be very large. In Fig. 4, the approximate sum rate for the high SNR regime from Corollary 1 is plotted versus the average SNR for different combinations of M. M is varied while κ is kept at 0.01 and α at 2.2. It is quite evident from the figure that at high SNR regime the path loss fluctuations are negated due to high transmit power of the users, thus producing very high sum rates. Also it can be seen that the simulations and approximations converge at relatively high SNR, which validates our analysis. As can be expected, $M = 8$ yields the maximum sum rate followed by other combinations. Furthermore, the slopes of the curves become steeper with the increase in M and the approximations converge with the simulations at very high SNR, thus validating our result.

In Fig. 5, we show the sum-rate approximation in the low SNR regime from Corollary 2. We consider similar settings as in Fig. 4 with the exception of the SNR range. Both simulations and analytic expression considering various M are plotted. The approximations effectively converge with the simulations for very low SNR while they diverge from the simulations in the moderately low SNR region. Moreover, it can be seen that the gap in performance when the number of antennas are increased is quite minimal. This is due to the fact that the multiplexing gains are lost in the low SNR regime.

At this point, it is worth mentioning the fact that the high and low SNR approximations are quite tight and considerably reduce the computation complexity of the sum rate of the system. From a system design point of view, they can be quite easy for engineers to implement in terms of computation time and complexity. Next, we analyze the EE of our system model with respect to a reference EE. We define this EE as relative EE. First, we calculate the EE of a reference system model and then simulate the EE of our system by normalizing it with the reference system model. We start by considering a SISO system with the single user equipped with a single-antenna transmitting

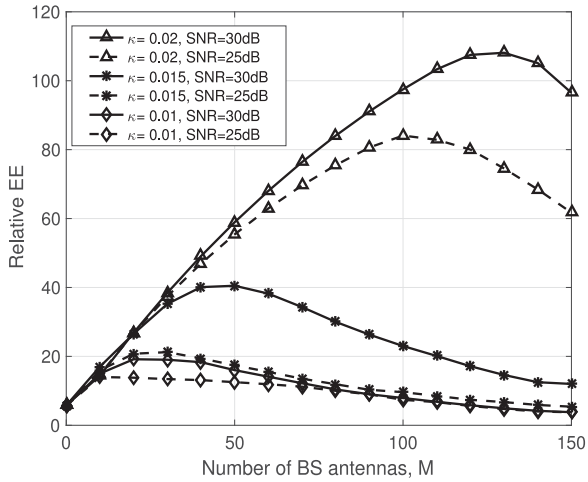

Fig. 6. Relative EE versus number of BS antennas, M with respect to a reference system ($M = 1$, $K = 1$, $n_k = 1$), for different SNR and user intensities. $\alpha = 2.2$.

to the BS equipped with one antenna only. We consider $P^{\text{BS}} = 1W$, $p^{\text{UE}} = 0.1$ W, and $p = 10$ dB. Thus from (24) we have

$$\xi_{\text{ref}} = \frac{\mathcal{R}_{M\,\text{ref}}}{p_{\text{ref}} + Mp^{\text{BS}} + Kp^{\text{UE}}}. \tag{29}$$

Numerically, we calculate $\mathcal{R}_{M\,\text{ref}} = 0.6$ bits/transmission for $M = 1$ and $K = 1$. Hence from (29), we get $\xi_{\text{ref}} = 0.054$ bits/J. The following EE discussion will be based on relative EE, defined as $\frac{\xi}{\xi_{\text{ref}}} = \frac{\xi}{0.054}$. Since it is a ratio, it is dimensionless. Fig. 6 illustrates the relative EE of the system with respect to M for different user intensities and transmit powers. For a particular transmit power, as we increase the number of antennas at the BS, the EE increases for a while, attains a local maximum, and then starts descending. This is an expected result as we consider a power consumption model, which is a function of M and K with respect to the circuit power consumption. Moreover, for a particular user intensity, with varying transmit power, the EE also increases in the beginning, attains a local maximum, and then starts decreasing. For example, for the case of $\kappa = 0.02$, the EE curves for SNR 25 and 30 dBs start falling between 100 and 150 antennas. This implies that a certain level of maximized EE can be achieved in such systems by increasing the number of BS antennas but with the important discrepancy of not requiring to increase the transmit power. In a nutshell, the EE curve is a quasi-concave function of M, which does not always increase with M in large MIMO systems.

At this point, it is worth mentioning the fact that the simulations results presented in this paper are comparable to recent massive MIMO literature. The sum-rate curves follow similar trend as seen in [8], [19], and [33]. The EE curves are also analogous to the ones presented in[2], [8], [23], and [33].

IX. Conclusion

The uplink performance of a massive MIMO system was analyzed. We use stochastic geometry to characterize the spatially distributed users while large dimensional RMT was used to achieve deterministic approximations of the sum rate of the system. We analyzed the sum rate of such a system both by means of simulations and analytical expressions. In particular, the BS along with the users were considered to follow a PPP. Approximations for the analytical sum rate were provided along with closed-form expressions at the low and high SNR regimes. The approximations were further validated with Monte Carlo simulations. The performances were evaluated with respect to the number of antennas at the BS and the intensity of the users. Analytical approximation for the rate of the general kth ordered user based on a PPP was derived. We also provided an analysis of the EE of the system by taking into consideration the circuit power consumption, which was shown to be a function of the number of antennas and the users. The relative EE of the system was plotted with respect to varying BS antennas for different SNR range. It was shown that the EE is a quasi-concave function of the number of BS antennas and does not always increase linearly with it.

Furthermore, the current work focuses on systems with simplified path loss models. In future, we will consider more complicated path loss models to get an even better analysis from a practical system implementation point of view. To meet the growing demands for data traffic, however, future cellular networks will be a mixture of high power macro base stations and lower power micro cells that will involve technologies such as mmWave. In such a scenario, it would be obligatory to consider LOS components. Thus, another direction for future work is to extend the current analysis for Rician faded channels. Moreover, to keep the analysis tractable, in this paper, we do not consider any complex detection techniques at the BS to separate the data streams. In future, we will consider complex detection techniques, such as zero forcing and minimum mean squared error at the BS on top of the current analysis.

Appendix A
Useful Lemmas

Lemma 2: Let $\Upsilon_k = \frac{M}{n_k}$ and $M, n_k \to \infty$, such that $0 < \min_k \liminf_M \Upsilon_k < \max_k \limsup_M \Upsilon_k < \infty$. Then, the deterministic equivalent of the uplink ergodic sum rate for a large antenna MIMO system consisting of M antennas and K users based on the Stieltjes and Shannon transform can be given as [19]

$$\bar{\mathcal{R}}_M(\rho) = \frac{1}{M}\log\det\left(\frac{\mathbf{\Gamma^{-1}}(\rho)}{\rho}\right) + \frac{1}{M}\sum_{k=1}^{K}\log\det\left(\frac{\tilde{\mathbf{\Delta}}^{\mathbf{-1}}(\rho)}{\rho}\right) - \rho\sum_{k=1}^{K}\varepsilon_k(\rho)\tilde{\varepsilon}_k(\rho), \tag{30}$$

where

$$\mathbf{\Gamma}(\rho) = \left(\mathbf{\Delta}(\rho)^{\mathbf{-1}} - \rho\tilde{\mathbf{H}}\tilde{\mathbf{\Delta}}(\rho)\tilde{\mathbf{H}}^{\mathbf{H}}\right)^{-1}, \tag{31}$$

$$\tilde{\mathbf{\Gamma}}(\rho) = \left(\tilde{\mathbf{\Delta}}(\rho)^{\mathbf{-1}} - \rho\tilde{\mathbf{H}}\mathbf{\Delta}(\rho)\tilde{\mathbf{H}}^{\mathbf{H}}\right)^{-1}, \tag{32}$$

$$\mathbf{\Delta}(\rho) = \frac{1}{\rho}\left(\mathbf{I}_M + \sum_{k=1}^{K}\tilde{\varepsilon}_k(\rho)\mathbf{R}_k\right), \tag{33}$$

$$\tilde{\mathbf{\Delta}}(\rho) = \frac{1}{\rho}\text{diag}\left(\mathbf{I}_{n_k} + \Upsilon_k \varepsilon_k(\rho)\mathbf{T}_k\right)_{\forall k}, \tag{34}$$

$$\varepsilon_k(\rho) = \frac{1}{M}\text{tr}(\mathbf{R}_k \mathbf{\Gamma}(\rho))_{\forall \mathbf{k}}, \tag{35}$$

$$\tilde{\varepsilon}_k(\rho) = \frac{1}{n_k}\text{tr}(\mathbf{T_k}\langle\tilde{\mathbf{\Gamma}}(\rho)\rangle_{\mathbf{k}})_{\forall \mathbf{k}}, \tag{36}$$

with $\tilde{\mathbf{H}}_k$ being the LOS channel between the BS and the user k and ρ the total SNR of the system.

Lemma 3: [34] A continuous function $f(x)$ converges if it is a contraction. Moreover, the continuous function $f(x)$ is a contraction if the absolute value of its first-order derivative is always less than 1.

APPENDIX B
PROOF OF PROPOSITION 1

Proof: For the case of Rayleigh faded channels with no LOS, Lemma 2 can be modified as

$$\hat{\mathcal{R}}_M(\rho) = \frac{1}{M}\log\det\left(\frac{\mathbf{\Lambda^{-1}}(\rho)}{\rho}\right) + \frac{1}{M}\sum_{k=1}^{K}\log\det\left(\frac{\tilde{\mathbf{\Lambda}}^{\mathbf{-1}}(\rho)}{\rho}\right) - \rho\sum_{k=1}^{K} e_k(\rho)\tilde{e}_k(\rho), \tag{37}$$

where

$$\mathbf{\Lambda}(\rho) = \frac{1}{\rho}\left(\mathbf{I}_M + \sum_{k=1}^{K}\tilde{\varepsilon}_k(\rho)\mathbf{R}_k\right), \tag{38}$$

$$\tilde{\mathbf{\Lambda}}(\rho) = \frac{1}{\rho}\text{diag}\left(\mathbf{I}_{n_k} + \frac{M}{n_k}\varepsilon_k(\rho)\mathbf{T}_k\right)_{\forall k}, \tag{39}$$

$$e_k(\rho) = \frac{1}{M}\text{tr}(\mathbf{R}_k\mathbf{\Lambda}(\rho))_{\forall \mathbf{k}}, \tag{40}$$

$$\tilde{e}_k(\rho) = \frac{1}{n_k}\text{tr}(\mathbf{T_k}\langle\tilde{\mathbf{\Lambda}}(\rho)\rangle_{\mathbf{k}})_{\forall \mathbf{k}}, \tag{41}$$

Therefore, simplifying (37)–(41) and incorporating the path losses for the users, which follow a PPP within the cell, the sum rate of a MIMO system can be approximated as

$$\mathcal{R}_M(\rho) = \frac{1}{M}\log\det\left(\mathbf{I}_M + \sum_{k\in\mathbf{\Phi(x)}}\tilde{\epsilon}_k(\rho)\mathbf{R}_k\right) + \mathbb{E}_{\mathbf{x}}\left\{\frac{1}{M}\sum_{k\in\mathbf{\Phi(x)}}\log\det\left(\mathbf{I}_{n_k} + \frac{M}{n_k}\mathcal{F}(\mathbf{x})\epsilon_k \times (\rho)\mathbf{T}_k\right)\right\} - \rho\sum_{k\in\mathbf{\Phi(x)}}\epsilon_k(\rho)\tilde{\epsilon}_k(\rho), \tag{42}$$

where $\epsilon_k(\rho)$ and $\tilde{\epsilon}_k(\rho)$ are as described in (15) and (16) and $\mathcal{F}$ denotes the large-scale fading as described before. Our aim now is to derive a closed form expression for the second term on the right-hand side of (42).

Let $\psi_k = \frac{M}{n_k}\epsilon_k(\rho)$. Then

$$\begin{aligned}
&\mathbb{E}_{\mathbf{x}}\left\{\log\det(\mathbf{I}_{n_k} + \mathcal{F}(\mathbf{x})\psi_k\mathbf{T}_k)\right\} \\
&= \frac{2}{r^2}\int_0^r \log\det(\mathbf{I}_{n_k} + \psi_k\mathbf{T}_k x^{-\alpha})x\mathrm{d}x \qquad (43)\\
&= \frac{2}{r^2}\int_0^r \log\prod_{i=1}^{n_k}(1+\psi_k\lambda_{ki}x^{-\alpha})x\mathrm{d}x \\
&= \frac{2}{r^2}\int_0^r \sum_{i=1}^{n_k}\log(1+\psi_k\lambda_{ki}x^{-\alpha})x\mathrm{d}x \\
&= \frac{2}{r^2\ln 10}\sum_{i=1}^{n_k}\int_0^r \ln(1+\psi_k\lambda_{ki}x^{-\alpha})x\mathrm{d}x \\
&= \frac{2}{r^2\ln 10}\sum_{i=1}^{n_k}\int_0^r G_{2,2}^{1,2}\left(\psi_k\lambda_{ki}\, x^{-\alpha}\Big|\begin{smallmatrix}1,1\\1,0\end{smallmatrix}\right)x\mathrm{d}x \\
&= \frac{2}{r^2\ln 10}\sum_{i=1}^{n_k}\int_0^r G_{2,2}^{2,1}\left(\frac{1}{\psi_k\lambda_{ki}}x^{\alpha}\Big|\begin{smallmatrix}0,1\\0,0\end{smallmatrix}\right)x\mathrm{d}x. \qquad (44)
\end{aligned}$$

Substituting y with x^α and changing the limits of integration, (44) becomes

$$\frac{2}{r^2\ln 10}\sum_{i=1}^{n_k}\int_0^{r^\alpha} G_{2,2}^{2,1}\left(\frac{1}{\psi_k\lambda_{ki}}y\Big|\begin{smallmatrix}0,1\\0,0\end{smallmatrix}\right)\frac{1}{\alpha}y^{(\frac{2}{\alpha}-1)}\mathrm{d}y. \tag{45}$$

Again, substituting z with $\frac{y}{r^\alpha}$ and changing the corresponding limits of integration, we have

$$\begin{aligned}
&\mathbb{E}_{\mathbf{x}}\left\{\log\det(\mathbf{I}_{n_k} + l(\mathbf{x})\psi_k\mathbf{T}_k)\right\} \\
&= \frac{2}{r^2\ln 10}\sum_{i=1}^{n_k}\int_0^1 G_{2,2}^{2,1}\left(\frac{r^\alpha}{\psi_k\lambda_{ki}}z\Big|\begin{smallmatrix}0,1\\0,0\end{smallmatrix}\right) \times \frac{1}{\alpha}\left(zr^\alpha\right)^{(\frac{2}{\alpha}-1)}r^\alpha\mathrm{d}z \\
&= \frac{2}{\alpha\ln 10}\sum_{i=1}^{n_k}\int_0^1 G_{2,2}^{2,1}\left(\frac{(r)^\alpha}{\psi_k\lambda_{ki}}z\Big|\begin{smallmatrix}0,1\\0,0\end{smallmatrix}\right)z^{(\frac{1}{\alpha}-1)}\mathrm{d}z \\
&= \frac{2}{\alpha\ln 10}\sum_{i=1}^{n_k}\Gamma(1)G_{3,3}^{2,2}\left(\frac{(r)^\alpha}{\psi_k\lambda_{ki}}\Big|\begin{smallmatrix}1-\frac{2}{\alpha},0,\ 1\\0,\quad 0,-\frac{2}{\alpha}\end{smallmatrix}\right). \qquad (46)
\end{aligned}$$

Plugging (46) in (42) and summing for k users (using Lemma 1), (14) is obtained. ■

APPENDIX C
PROOF OF UNIQUENESS OF (15) AND (16)

In order to prove that $\epsilon_k(\rho)$ and $\tilde{\epsilon}_k(\rho)$ have unique solutions, it is sufficient to show that after a single update or an iteration, $\epsilon_k(\rho)$ and $\tilde{\epsilon}_k(\rho)$ converge. We will use the contraction principle [34] to show that $\epsilon_k^{t+1}(\rho) - \epsilon_k^t(\rho) \to 0$ and $\tilde{\epsilon}_k^{t+1}(\rho) - \tilde{\epsilon}_k^t(\rho) \longrightarrow 0$, where t is any instant. Now at instant

$t+1$, (15) and (16) can be given as

$$\epsilon_k^{t+1}(\rho) = \frac{1}{M}\mathrm{tr}\left(\rho\mathbf{R}_k\left[\mathbf{I}_M + \sum_{k=0}^{\infty}\tilde{\epsilon}_k^t(\rho)\mathbf{R}_k\ \mathbb{P}(k)\right]^{-1}\right) \quad (47)$$

$$\tilde{\epsilon}_k^{t+1}(\rho) = \frac{1}{n_k}\mathrm{tr}\left(\rho\mathbf{T}_k\left\langle \mathrm{diag}\left[\mathbf{I}_{n_k} + \frac{M\epsilon_k^t(\rho)\mathbf{T}_k}{n_k}\right]^{-1}_{\forall k\in\mathbf{\Phi}(\mathbf{x})}\right\rangle\right). \quad (48)$$

We assume that $\lambda_i(\mathbf{A})$ is the ith eigenvalue of the matrix $\mathbf{A}$. Without loss of generality, the $\lambda_i(\mathbf{A})$s are sorted in nonincreasing order as $\lambda_1(\mathbf{A}) \geq \lambda_2(\mathbf{A}) \geq \lambda_3(\mathbf{A}) \geq \cdots$. Herein, (47) and (48) are equivalent to [35]

$$\epsilon_k^{t+1}(\rho) = \frac{1}{M}\sum_{i=1}^{M}\frac{\lambda_i(\rho\mathbf{R})}{1+\lambda_i\left(\sum_{k=0}^{\infty}\tilde{\epsilon}_k^t(\rho)\mathbf{R}\right)\mathbb{P}(k)} \quad (49)$$

$$\tilde{\epsilon}_k^{t+1}(\rho) = \frac{1}{n_k}\sum_{i=1}^{n_k}\frac{\lambda_i(\rho\mathbf{T}_k)}{1+\lambda_i\left(\frac{M\epsilon_k^t(\rho)}{n_k}\mathbf{T}_k\right)}. \quad (50)$$

It should be noted that, in our model, we assume the correlation matrices at the BS, $\mathbf{R}_k$s to be all the same and hence without loss of generality, we write $\mathbf{R}_k = \mathbf{R}$. Furthermore, let

$$\Psi_k^t = \frac{1}{n_k}\left(1 + \frac{1}{\epsilon_k^t(\rho)}\sum_{i=1}^{n_k}\frac{1}{\lambda_i(\mathbf{T}_k)}\right). \quad (51)$$

Then, the eigenvalues of matrix $\mathbf{T}_k$ is given by

$$\lambda_i(\mathbf{T}_k) = \left(\Psi_k^t\lambda_i(\mathbf{T}_k) - \left(\epsilon_k^t(\rho)\right)^{-1}\right)_+, \quad (52)$$

where $(\mathbf{A})_+$ is the element-wise positive part of matrix $(\mathbf{A})$, while for scalar $(x)_+ \triangleq \max\{0, x\}$. With the help of (51) and (52), $\tilde{\epsilon}_k^{t+1}(\rho)$ can now be rewritten as

$$\begin{aligned}\tilde{\epsilon}_k^{t+1}(\rho) &= \frac{\rho}{n_k}\sum_{i=1}^{n_k}\frac{\Psi_k^t\lambda_i(\mathbf{T}_k) - (\epsilon_k^t(\rho))^{-1}}{\frac{M}{n_k}\epsilon_k^t(\rho)\Psi_k^t\lambda_i(\mathbf{T}_k)}\\ &= \frac{\rho}{\epsilon_k^t(\rho)\Psi_k^t M}\\ &= \frac{\rho\frac{n_k}{M}}{\epsilon_k^t(\rho) + \sum_{i=1}^{n_k}\frac{1}{\lambda_i(\mathbf{T}_k)}}. \end{aligned} \quad (53)$$

Letting $v_k^t = \ln(\tilde{\epsilon}_k^t(\rho))$, the convergence problem of $\epsilon_k^{t+1}(\rho)$ and $\tilde{\epsilon}_k^{t+1}(\rho)$ is equivalent to the convergence problem of the following function:

$$v_k^{t+1} = f(v_k^{t-1}), \quad (54)$$

where $f(v_k^{t-1})$ can be written as (55), shown at the bottom of this page.

In the following, we will proof that the function $f(v_k^{t-1})$ convergences. First, we note that the function $f(v_k^{t-1})$ is obviously continuous. Second, we compute the first derivative of $f(v_k^{t-1})$, which is given by (56), shown at the bottom of this page.

At this point, it is obvious that

$$\frac{e^{v_k^{t-1}}}{\frac{1}{\lambda_i(\mathbf{R})} + \sum_{j=0,\ j\neq k}^{\infty}\tilde{\epsilon}_j^{t-1}(\rho)\mathbb{P}(j) + e^{v_k^{t-1}}} \leq 1. \quad (57)$$

Accordingly, we derive (58), shown at the top of the next page, from (56) and (57).

It is easy to show that the first derivative of $f(v_k^{t-1})$ is also positive, which means that the absolute value of $f'(v_k^{t-1})$ is smaller than 1. Hence, using Lemma 3, we can state that $f(v_k^{t-1})$ is a contraction, which implies that it converges. This concludes the proof of uniqueness of (15) and (16).[6]

[6]For the special case, when a single user is considered, a similar proof of convergence was shown in [35].

$$\begin{aligned} f(v_k^{t-1}) &= \ln\left(\frac{\rho n_k}{M}\right) - \ln\left(\frac{1}{M}\sum_{i=1}^{M}\frac{\lambda_i(\rho\mathbf{R})}{1+\lambda_i\left(\sum_{k=0}^{\infty}\tilde{\epsilon}_k^{t-1}(\rho)\mathbf{R}\ \mathbb{P}(k)\right)} + \sum_{i=1}^{n_k}\frac{1}{\lambda_i(\mathbf{T}_k)}\right)\\ &= \ln\left(\frac{\rho n_k}{M}\right) - \ln\left(\frac{1}{M}\sum_{i=1}^{M}\frac{\lambda_i(\rho\mathbf{R})}{1+\sum_{j=0,\ j\neq k}^{\infty}\tilde{\epsilon}_j^{t-1}(\rho)\lambda_i(\mathbf{R})\ \mathbb{P}(j) + e^{v_k^{t-1}}\lambda_i(\mathbf{R})} + \sum_{i=1}^{n_k}\frac{1}{\lambda_i(\mathbf{T}_k)}\right)\\ &= \ln\left(\frac{\rho n_k}{M}\right) - \ln\left(\frac{1}{M}\sum_{i=1}^{M}\frac{\rho}{\frac{1}{\lambda_i(\mathbf{R})} + \sum_{j=0,\ j\neq k}^{\infty}\tilde{\epsilon}_j^{t-1}(\rho)\ \mathbb{P}(j) + e^{v_k^{t-1}}} + \sum_{i=1}^{n_k}\frac{1}{\lambda_i(\mathbf{T}_k)}\right) \end{aligned} \quad (55)$$

$$f'(v_k^{t-1}) = \frac{\sum_{i=1}^{M}\frac{\rho e^{v_k^{t-1}}}{\left(\frac{1}{\lambda_i(\mathbf{R})} + \sum_{j=0,\ j\neq k}^{\infty}\tilde{\epsilon}_j^{t-1}(\rho)\ \mathbb{P}(j) + e^{v_k^{t-1}}\right)^2}}{\sum_{i=1}^{M}\frac{\rho}{\frac{1}{\lambda_i(\mathbf{R})} + \sum_{j=0,\ j\neq k}^{\infty}\tilde{\epsilon}_j^{t-1}(\rho)\ \mathbb{P}(j) + e^{v_k^{t-1}}} + M\sum_{i=1}^{n_k}\frac{1}{\lambda_i(\mathbf{T}_k)}} \quad (56)$$

$$f^{'}(v_k^{t-1}) \leq \frac{\sum_{i=1}^{M} \dfrac{\rho}{\dfrac{1}{\lambda_i(\mathbf{R})} + \sum\limits_{j=0,\ j\neq k}^{\infty} \tilde{\epsilon}_j^{t-1}(\rho)\ \mathbb{P}(j) + e^{v_k^{t-1}}}}{\sum_{i=1}^{M} \dfrac{\rho}{\dfrac{1}{\lambda_i(\mathbf{R})} + \sum\limits_{j=0,\ j\neq k}^{\infty} \tilde{\epsilon}_j^{t-1}(\rho)\ \mathbb{P}(j) + e^{v_k^{t-1}}} + M\sum_{i=1}^{n_k} \dfrac{1}{\lambda_i(\mathbf{T}_k)}} \leq 1 \tag{58}$$

APPENDIX D
PROOF OF PROPOSITION 2

Proof: Let $\psi_k = \frac{M}{n_k}\epsilon_k(\rho)$. Then using (20)

$$\begin{aligned}
&\mathbb{E}_{\mathbf{x}}\left\{\log\det(\mathbf{I}_{n_k} + \mathcal{F}(\mathbf{x}_k)\psi_k\mathbf{T}_k)\right\} \\
&= \frac{2\kappa\pi}{\Gamma(k)}\sum_{i=1}^{n_k}\int_0^r \log(1+\psi_k\lambda_{ki}x^{-\alpha})\exp(-\kappa\pi x^2)x^{2k}\mathrm{d}x \\
&= \frac{2\kappa\pi}{\Gamma(k)}\sum_{i=1}^{n_k}\int_0^r G_{2,2}^{2,1}\left(\frac{1}{\psi_k\lambda_{ki}}x^{\alpha}\middle|\begin{matrix}0,1\\0,0\end{matrix}\right)\exp(-\kappa\pi x^2)x^{2k}\mathrm{d}x.
\end{aligned} \tag{59}$$

Substituting y with $x\sqrt{\kappa\pi}$ and changing the limits of integration, (59) becomes

$$\begin{aligned}
&\frac{2}{\Gamma(k)}\sum_{i=1}^{n_k}\int_0^{r\sqrt{\kappa\pi}} G_{2,2}^{2,1}\left(\frac{1}{(\kappa\pi)^{\frac{\alpha}{2}}\psi_k\lambda_{ki}}y^{\alpha}\middle|\begin{matrix}0,1\\0,0\end{matrix}\right) \\
&\quad\times\exp(-y^2)\frac{y^{2k}}{(\sqrt{\kappa\pi})^{(k+1)}}\mathrm{d}y.
\end{aligned} \tag{60}$$

Now, expanding $\exp(-y^2)$ with the help of Taylor's series expansion, we have

$$\exp(-y^2) = \sum_{n=0}^{\infty}(-1)^n\frac{y^{2n}}{n!}. \tag{61}$$

Furthermore, using (61) in (34), we have

$$\begin{aligned}
&\frac{2\sum_{n=0}^{\infty}(-1)^n}{n!\Gamma(k)(\sqrt{\kappa\pi})^{(k+1)}}\sum_{i=1}^{n_k}\int_0^{r\sqrt{\kappa\pi}} G_{2,2}^{2,1} \\
&\quad\cdot\left(\frac{1}{(\kappa\pi)^{\frac{\alpha}{2}}\psi_k\lambda_{ki}}y^{\alpha}\middle|\begin{matrix}0,1\\0,0\end{matrix}\right)y^{2(n+k)}\mathrm{d}y.
\end{aligned} \tag{62}$$

Substituting z with $\frac{y}{\sqrt{\kappa\pi r}}$ and changing the limits of integration, (62) becomes

$$\begin{aligned}
&\frac{2\sum_{n=0}^{\infty}(-1)^n(\sqrt{\kappa\pi})^{(2n+k)}r^{(2(n+k)+1)}}{n!\Gamma(1)} \\
&\quad\times\sum_{i=1}^{n_k}\int_0^1 G_{2,2}^{2,1}\left(\frac{r^{\alpha}}{\psi_k\lambda_{ki}}z^{\alpha}\middle|\begin{matrix}0,1\\0,0\end{matrix}\right)z^{2(n+k)}\mathrm{d}z.
\end{aligned} \tag{63}$$

Simplifying (63) we get

$$\begin{aligned}
&\frac{2\sum_{n=0}^{\infty}(-1)^n(\sqrt{\kappa\pi})^{(2n+k)}r^{(2(n+k)+1)}}{\alpha n!\Gamma(k)} \\
&\quad\times\sum_{i=1}^{n_k}\int_0^1 G_{2,2}^{2,1}\left(\frac{r^{\alpha}}{\psi_k\lambda_{ki}}z^{\alpha}\middle|\begin{matrix}0,1\\0,0\end{matrix}\right)p^{\left(\frac{2(n+k)+1}{\alpha}-1\right)}\mathrm{d}p.
\end{aligned} \tag{64}$$

From (64), we have $\rho = \frac{2(n+k)+1}{\alpha}$, $\sigma = 1$, and $\chi = \frac{r^{\alpha}}{\lambda_{ki}}$. Hence (64) can be approximated as

$$\begin{aligned}
&\frac{2\sum_{n=0}^{\infty}(-1)^n(\sqrt{\kappa\pi})^{(2n+k)}r^{(2(n+k)+1)}}{\alpha n!\Gamma(k)} \\
&\quad\times\Gamma(1)\sum_{i=1}^{n_k}G_{3,3}^{2,2}\left(\frac{r^{\alpha}}{\psi_k\lambda_{ki}}\middle|\begin{matrix}1-\frac{2(n+k)+1}{\alpha},0,\ 1\\0,\quad 0,-\frac{2(n+k)+1}{\alpha}\end{matrix}\right).
\end{aligned} \tag{65}$$

Plugging (65) into (42) for the kth user, we get (21). ■

REFERENCES

[1] V. Jungnickel *et al.*, "The role of small cells, coordinated multipoint, and massive MIMO in 5G," *IEEE Commun. Mag.*, vol. 52, no. 5, pp. 44–51, May 2014.

[2] E. Larsson, O. Edfors, F. Tufvesson, and T. Marzetta, "Massive MIMO for next generation wireless systems," *IEEE Commun. Mag.*, vol. 52, no. 2, pp. 186–195, Feb. 2014.

[3] J. Hoydis, S. ten Brink, and M. Debbah, "Massive MIMO in the UL/DL of cellular networks: How many antennas do we need?" *IEEE J. Sel. Areas Commun.*, vol. 31, no. 2, pp. 160–171, Feb. 2013.

[4] L. Lu, G. Li, A. Swindlehurst, A. Ashikhmin, and R. Zhang, "An overview of massive MIMO: Benefits and challenges," *IEEE J. Sel. Topics Signal Process.*, vol. 8, no. 5, pp. 742–758, Oct. 2014.

[5] F. Rusek *et al.*, "Scaling up MIMO: Opportunities and challenges with very large arrays," *IEEE Commun. Mag.*, vol. 30, no. 1, pp. 40–60, Jan. 2013.

[6] F. Boccardi, R. Heath, A. Lozano, T. Marzetta, and P. Popovski, "Five disruptive technology directions for 5G," *IEEE Commun. Mag.*, vol. 52, no. 2, pp. 74–80, Feb. 2014.

[7] T. Marzetta, "Noncooperative cellular wireless with unlimited numbers of base station antennas," *IEEE Trans. Wireless Commun.*, vol. 9, no. 11, pp. 3590–3600, Nov. 2010.

[8] H. Q. Ngo, E. Larsson, and T. Marzetta, "Energy and spectral efficiency of very large multiuser MIMO systems," *IEEE Trans. Commun.*, vol. 61, no. 4, pp. 1436–1449, Apr. 2013.

[9] H. Q. Ngo, E. Larsson, and T. Marzettat, "Uplink power efficiency of multiuser MIMO with very large antenna arrays," in *Proc. Annu. Allerton Conf. Commun. Control, Comput.*, Sep. 2011, pp. 1272–1279.

[10] A. M. Tulino and S. Verdu, "Random matrix theory and wireless communications," *Found. Trends Commun. Inf. Theory*, vol. 1, no. 1, pp. 1–182, 2004.

[11] G. J. Foschini and M. J. Gans, "On limits of wireless communications in a fading environment when using multiple antennas," *Wireless Pers. Commun.*, vol. 6, pp. 311–335, 1998.

[12] E. Telatar, "Capacity of multi-antenna Gaussian channels," *Eur. Trans. Telecommun.*, vol. 10, no. 6, pp. 585–595, 1999.

[13] S. Verdu and S. Shamai, "Spectral efficiency of CDMA with random spreading," *IEEE Trans. Inf. Theory*, vol. 45, no. 2, pp. 622–640, Mar. 1999.

[14] P. Rapajic and D. Popescu, "Information capacity of a random signature multiple-input multiple-output channel," *IEEE Trans. Commun.*, vol. 48, no. 8, pp. 1245–1248, Aug. 2000.

[15] J. Xue, T. Ratnarajah, C. Zhong, and C. Wen, "Reliability analysis for large MIMO systems," *IEEE Wireless Commun. Lett.*, vol. 3, no. 6, pp. 553–556, Dec. 2014.

[16] A. Lozano and A. Tulino, "Capacity of multiple-transmit multiple-receive antenna architectures," *IEEE Trans. Inf. Theory*, vol. 48, no. 12, pp. 3117–3128, Dec. 2002.

[17] C.-N. Chuah, D. Tse, J. Kahn, and R. Valenzuela, "Capacity scaling in MIMO wireless systems under correlated fading," *IEEE Trans. Inf. Theory*, vol. 48, no. 3, pp. 637–650, Mar. 2002.

[18] R. Couillet, M. Debbah, and J. Silverstein, "A deterministic equivalent for the analysis of correlated MIMO multiple access channels," *IEEE Trans. Inf. Theory*, vol. 57, no. 6, pp. 3493–3514, Jun. 2011.

[19] J. Zhang, C.-K. Wen, S. Jin, X. Gao, and K.-K. Wong, "On capacity of large-scale MIMO multiple access channels with distributed sets of correlated antennas," *IEEE J. Sel. Areas Commun.*, vol. 31, no. 2, pp. 133–148, Feb. 2013.

[20] H. ElSawy, E. Hossain, and M. Haenggi, "Stochastic geometry for modeling, analysis, and design of multi-tier and cognitive cellular wireless networks: A survey," *IEEE Commun. Surveys Tut.*, vol. 15, no. 3, pp. 996–1019, Mar. 2013.

[21] S. Cui, A. Goldsmith, and A. Bahai, "Energy-efficiency of MIMO and cooperative MIMO techniques in sensor networks," *IEEE Trans. Sel. Areas Commun.*, vol. 22, no. 6, pp. 1089–1098, Aug. 2004.

[22] S. Tombaz, A. Vastberg, and J. Zander, "Energy and cost-efficient ultra-high-capacity wireless access," *IEEE Trans. Wireless Commun.*, vol. 18, no. 5, pp. 18–24, Oct. 2011.

[23] D. Ha, K. Lee, and J. Kang, "Energy efficiency analysis with circuit power consumption in massive MIMO systems," in *Proc. IEEE Int. Symp. Per. Indoor Mobile Radio Commun.*, Sep. 2013, pp. 938–942.

[24] E. Bjornson, L. Sanguinetti, J. Hoydis, and M. Debbah, "Designing multi-user MIMO for energy efficiency: When is massive MIMO the answer?" in *Proc. IEEE Wireless Commun. Netw. Conf.*, Apr. 2014, pp. 242–247.

[25] T. Ratnarajah and R. Vaillancourt, "Quadratic forms on complex random matrices and multiple-antenna systems," *IEEE Trans. Inf. Theory*, vol. 51, no. 8, pp. 2976–2984, Aug. 2005.

[26] A. Goldsmith, S. Jafar, N. Jindal, and S. Vishwanath, "Capacity limits of MIMO channels," *IEEE J. Sel. Areas Commun.*, vol. 21, no. 5, pp. 684–702, Jun. 2003.

[27] A. L. Moustakas, S. H. Simon, and A. M. Sengupta, "MIMO capacity through correlated channels in the presence of correlated interferers and noise: A (not so) large N analysis," *IEEE Trans. Inf. Theory*, vol. 49, no. 10, pp. 2545–2561, Oct. 2003.

[28] M. Haenggi, "On distances in uniformly random networks," *IEEE Trans. Inf. Theory*, vol. 51, no. 10, pp. 3584–3586, Oct. 2005.

[29] A. Jeffrey and D. Zwillinger, *Table of Integrals, Series, and Products*, 6th ed. San Diego, CA, USA: Academic, 2000.

[30] E. V. A. Schönhage and A.F.W. Grotefeld, *Fast Algorithms—A Multitape Turing Machine Implementation*. Mannheim, Germany: B.I. Wissenschafts-Verlag, 1994.

[31] P. B. B. Jonathan and M. Borwein, *A Study in Analytic Number Theory and Computational Complexity*. New York, NY, USA: Wiley, 1998.

[32] Y. Chen, S. Zhang, S. Xu, and G. Li, "Fundamental trade-offs on green wireless networks," *IEEE Commun. Mag.*, vol. 49, no. 6, pp. 30–37, Jun. 2011.

[33] S. Biswas, C. Masouros, and T. Ratnarajah, "Performance analysis of large multi-user MIMO systems with space-constrained 2D antenna arrays," *IEEE Trans. Wireless Commun.*, vol. 15, no. 5, pp. 3492–3505, May 2016. doi: 10.1109/TWC.2016.2522419.

[34] W. Rudin, *Principles of Mathematical Analysis*, 3rd ed. New York, NY, USA: McGraw-Hill, 1976.

[35] G. Taricco and E. Riegler, "On the ergodic capacity of correlated Rician fading MIMO channels with interference," *IEEE Trans. Inf. Theory*, vol. 57, no. 7, pp. 4123–4137, Jul. 2011.

Sudip Biswas (S'16) received the B.Tech. degree in electronics and communication engineering from the Sikkim Manipal Institute of Technology, Sikkim, India, in 2010, and the M.Sc. degree in signal processing and communications from the University of Edinburgh, Edinburgh, U.K., in 2013. He is currently working toward the Ph.D. degree in digital communications at the Institute for Digital Communications, University of Edinburgh, Edinburgh, U.K.

His research interests include various topics in wireless communications and network information theory with particular focus on stochastic geometry and possible 5G technologies such as massive MIMO, mmWave, and full-duplex.

Jiang Xue (S'09–M'13) received the B.S. degree in information and computing science from Xi'an Jiaotong University, Xi'an, China, in 2005, the M.S. degree in applied mathematics from Lanzhou University, Lanzhou, China, in 2009, the M.S. degree in applied mathematics from Uppsala University, Uppsala, Sweden, in 2009, and the Ph.D. degree in electrical and electronic engineering from ECIT, Queen's University of Belfast, Belfast, U.K., in 2012.

He is currently a Research Fellow with the University of Edinburgh, Edinburgh, U.K. His main interests include the performance analysis of general multiple antenna systems, stochastic geometry, cooperative communications, and cognitive radio.

Faheem A. Khan (M'02) received the Ph.D. degree in electrical and electronic engineering from Queen's University Belfast, Belfast, U.K., in 2012.

He is currently a Research Associate in wireless communications and signal processing with the Institute for Digital Communications, University of Edinburgh, Edinburgh, U.K., under the EU funded FP7 project ADEL. He has been actively involved in the past EU FP7 projects CROWN, HIATUS, and HARP. His research interests include cognitive radio networks, licensed shared access, 5G wireless networks, millimeter-wave communications, and cooperative communications.

Tharmalingam Ratnarajah (A'96–M'05–SM'05) is currently with the Institute for Digital Communications, University of Edinburgh, Edinburgh, U.K., as a Professor of digital communications and signal processing. He has authored or coauthored more than 270 publications. He holds four U.S. patents. He is currently the Coordinator of the FP7 projects HARP (3.2M€) in the area of highly distributed MIMO and ADEL (3.7M€) in the area of licensed shared access. Previously, he was the Coordinator of FP7 Future and Emerging Technologies project CROWN (2.3M€) in the area of cognitive radio networks and HIATUS (2.7M€) in the area of interference alignment. His research interests include signal processing and information theoretic aspects of 5G wireless networks, full-duplex radio, mmWave communications, random matrices theory, interference alignment, statistical and array signal processing, and quantum information theory.

Prof. Ratnarajah is a Fellow of the Higher Education Academy, U.K. He is an Associate Editor of the IEEE TRANSACTIONS ON SIGNAL PROCESSING.